

Star formation and nuclear activity in close pairs of early-type galaxies

Ben Rogers¹, Ignacio Ferreras^{2*}, Sugata Kaviraj^{2,3}, Anna Pasquali⁴ and Marc Sarzi⁵

¹ *Department of Physics, King's College London, Strand, London WC2R 6LS*

² *Mullard Space Science Laboratory, University College London, Holmbury St Mary, Dorking, Surrey RH5 6NT*

³ *Department of Physics, Denys Wilkinson Building, Oxford, OX1 3RH*

⁴ *Max-Planck-Institut für Astronomie, Königstuhl 17, D-69117 Heidelberg, Germany*

⁵ *Centre for Astrophysics Research, University of Hertfordshire, College Lane, Hatfield, Herts AL10 9AB*

MNRAS, Accepted 2009 July 19. Received 2009 July 03; in original form 2009 May 11

ABSTRACT

We extract from the Sloan Digital Sky Survey a sample of 347 systems involving early type galaxies separated by less than 30 kpc, in projection, and 500 km/s in radial velocity. These close pairs are likely progenitors of dry mergers. The (optical) spectra is used to determine how the interaction affects the star formation history and nuclear activity of the galaxies. The emission lines (or lack thereof) are used to classify the sample into AGN, star forming or quiescent. Increased AGN activity and reduced star formation in early-type pairs that already appear to be interacting indicate that the merging process changes the nature of nebular activity, a finding that is also supported by an increase in AGN luminosity with decreasing pair separation. Recent star formation is studied on the absorption line spectra, both through principal component analysis as well as via a comparison of the spectra with composite stellar population models. We find that the level of recent star formation in close pairs is raised relative to a control sample of early-type galaxies. This excess of residual star formation is found throughout the sample of close pairs and does not correlate with pair separation or with visual signs of interaction. Our findings are consistent with a scenario whereby the first stage of the encounter (involving the outer parts of the halos) trigger residual star formation, followed by a more efficient inflow towards the centre – switching to an AGN phase – after which the systems are quiescent.

Key words: galaxies: elliptical and lenticular, cD – galaxies: evolution – galaxies: formation – galaxies: stellar content.

1 INTRODUCTION

It is well known that early type galaxies are dominated by old stellar populations (see e.g. Kodama & Arimoto 1997; Stanford et al. 1998). It has also been shown through studies of NUV photometry from GALEX (Yi et al. 2005; Kaviraj et al. 2007) as well as statistical dissections of the optical spectra (Ferreras et al. 2006; Rogers et al. 2007; Nolan et al. 2007) that a large fraction of early types have undergone small amounts of recent star formation. However there is less certainty as to the cause of this recent star formation. One possible scenario involves minor mergers from small blobs of gas surrounding the galaxy (Kaviraj 2008; Kaviraj et al. 2009). In that case, the young stellar mass content will be roughly independent of galaxy mass, which implies recent star formation will be more readily detectable in lower mass early-types, as observed. This scenario will also result in enhanced recent star for-

mation within close pairs, where these small pockets of gas could be disrupted during the encounter. In this paper we study differences in the spectroscopic data of close pairs involving only early-type galaxies with the aim of understanding the connection between galaxy interactions and star formation or AGN activity. Restricting the selection to pairs involving only early-types (i.e. precursors of dry mergers) results in a cleaner sample, minimising the contamination from gas in the interaction process.

Within the standard framework of a Λ CDM cosmology, elliptical galaxies are formed through the merger of many smaller systems (see e.g. De Lucia et al. 2005) and although the build up of the red population occurs mainly at high redshift (e.g. Bundy et al. 2005; Ferreras et al. 2009), signs of previous merging events are found in early-type systems, such as kinematically decoupled cores (Davies et al. 2001; McDermid et al. 2006), distorted morphologies, shells and other fine structure (van Dokkum 2005).

The overall old stellar populations found in elliptical galaxies can be used to constrain the time since the last major episode

* E-mail: ferreras@star.ucl.ac.uk

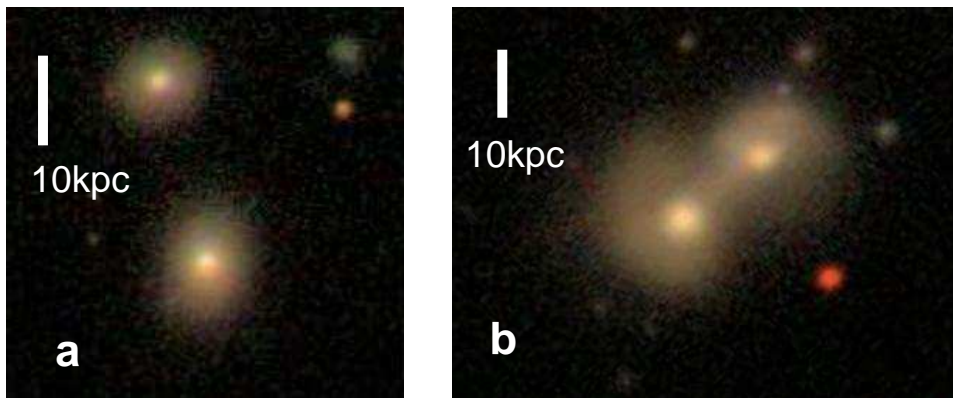


Figure 1. An example of close pairs of SDSS early-type galaxies used in this paper: Non-interacting (a; SDSS J101434.27-005013.1; $z=0.045$) vs. interacting (b; SDSS J083645.89+472210.1; $z=0.053$). The vertical bar represents a projected distance of 10 kpc.

of star formation. If the last merger involved late type galaxies, it must have taken place at early times, otherwise the resulting young populations would be seen in a photometric/spectroscopic analysis. However, if the last merger involves gas poor galaxies, one could still accommodate mergers at late times. It has been shown that models describing the formation of massive elliptical galaxies require a nondissipative merger (i.e. limited amounts of cold gas) to recreate the dynamics of the largest ellipticals, such as boxy isophotes and minimal rotation (Naab et al. 2006), (although see Kang et al. 2007). Therefore it is reasonable to assume that the last merger for a significant fraction of ellipticals involved early-type galaxies as progenitors (Khochfar & Burkert 2003).

Given the large fraction of elliptical galaxies likely to contain small but significant amounts of cold gas (Knapp et al. 1989; Young 2005), disruption of this gas via gravitational interactions/harassment or through ‘dry’ mergers may well result in small amounts of star formation. It is also worth considering that previous work (Ferreras et al. 2006; Rogers et al. 2007) has indicated that recent star formation may be more significant in medium density environments, implying that galaxy harassment may be efficient at stimulating small episodes of star formation.

In this paper we investigate these possibilities by looking at *elliptical only* close pairs. We analyse the emission spectra to identify active galaxies (AGN or star forming) and explore whether the impending merger affects the nature of the activity. We also perform a comprehensive analysis of the stellar populations, using two independent methods: principal component analysis, and a maximum likelihood analysis involving a grid of models. The latter uses a number of age and metallicity sensitive spectral features measured via a new estimator of equivalent width that minimises the contamination from neighbouring lines (Rogers et al. 2008).

2 THE CLOSE PAIRS SAMPLE

Our classification starts with an initial sample of ~ 3000 galaxies in close pair systems from the Sloan Digital Sky Survey (SDSS) DR6 database (Adelman-McCarthy et al. 2008). A close pair is defined as a system of two or more galaxies within a projected physical distance of 30 kpc and with relative velocity below 500 km/s (i.e. $\Delta z = 0.0017$). The choice is motivated by previous work on the presence of interaction signs in close pairs of SDSS galaxies (see e.g. Patton et al. 2000).

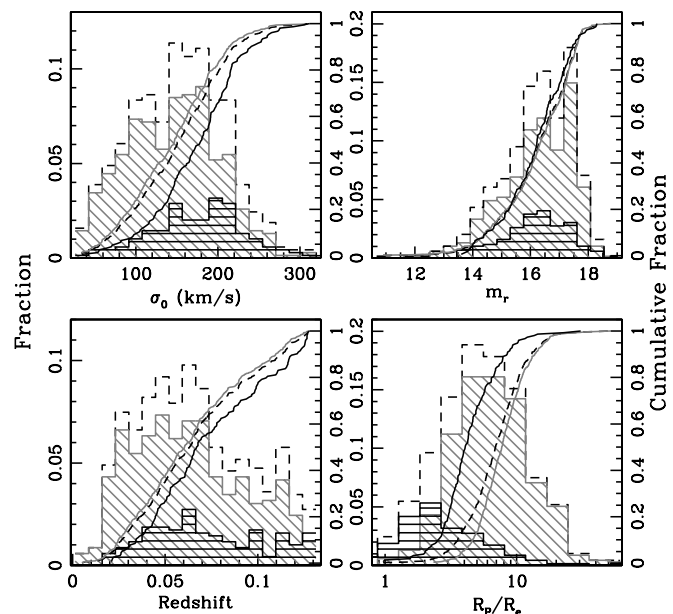


Figure 2. The distribution of the sample is shown in terms of redshift (*bottom left*), central velocity dispersion, σ_0 (*top left*), apparent r-band magnitude (*top right*) and the ratio between the projected separation of the pair and the half-light radius, R_p/R_e (*bottom right*). The histograms show the distributions of the pairs depending on whether the system is visually classified as interacting (black solid) or not (grey). The full sample corresponds to the black dashed lines. Overplotted are the cumulative distributions (with the same colour coding) which highlight differences between the two types of pairs.

We make a visual classification of this sample using r-band FITS stamps retrieved from the SDSS pipeline. The morphology of each system of galaxies was estimated by eye by B. R., I. F., S. K. and A. P. In order to simplify the classification method, we bin the systems into three types: non-early type, lenticular or elliptical. We emphasize that our sample targets systems where *both* galaxies are early-types. Non-early type systems are those which show one or more galaxies with structure characteristic of a late-type: a dominant disk component or spiral arms. Lenticulars and ellipticals are

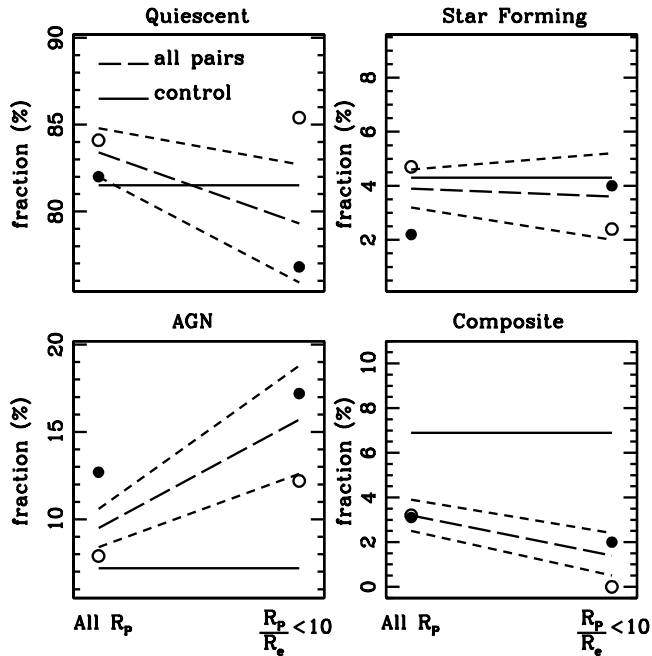


Figure 3. The variation of emission line activity with respect to pair separation is shown for our sample of close pairs (dashed lines, including Poissonian error bars) and for a control sample of SDSS early-type galaxies from Schawinski et al. (2007a, solid lines). For each panel, the left (right) side of the box corresponds to all galaxies (galaxies separated from the other member by less than 10 times the half-light radius). The filled (open) circles correspond to galaxies visually classified as interacting (non-interacting). This figure illustrates the fractions shown in table 1.

defined as bulge-dominated galaxies with or without a visible disk component, respectively. This classification resulted in a sample of 346 early-type only pairs and one triplet system, comprising 695 galaxies in total.

These pairs were further divided into categories, based on the estimated level of interaction occurring within the system. This scheme is similar to previous classifications (see Alonso et al. 2007), although we only consider two cases. Our systems are either “non interacting” or “interacting” depending on whether the close pair shows tidal tails or other distortions, indicating a significant level of interaction. Figure 1 shows an example of each type. This criterion is also determined by a majority selection from the four classifiers. Systems for which there was an equal split between classifiers was considered as “non interacting”.

Optical spectra for the entire sample were retrieved from the SDSS DR6 and processed using the PPXF and GANDALF codes (Cappellari & Emsellem 2004; Sarzi et al. 2006), adapted for fitting SDSS data. These codes provide stellar kinematics and emission line luminosities by simultaneously fitting both stellar population models (Tremonti et al. 2004) and gaussian emission line templates. The latter – when present – allow us to determine the nature of the ionising source. A comparison of the Balmer decrement ($H\alpha/H\beta$) to standard case B recombination (Osterbrock & Ferland 2006) is used to correct for the effect of internal dust by using the extinction law of Calzetti et al. (2000). The emission spectra is removed from the observed data to determine the original SED of the underlying stellar populations. This is an important point when

comparing the equivalent widths of absorption features with synthetic models in order to constrain the star formation history (SFH).

Figure 2 shows the general properties of our early-type close pairs sample. The histograms are coded with respect to the interaction type: non-interacting systems are shown in grey, and interacting pairs are shown in black. The full sample is shown as a dashed histogram. We include in the figure the cumulative distributions to help assess the difference between samples. We draw attention to the central velocity dispersion (σ_0 ; top-left), whose distribution is slightly biased towards higher values for interacting galaxies, as expected (Park & Choi 2009). We note that a similar trend was found by Alonso et al. (2007), who showed that the estimated black hole mass, derived from the σ_0 -BH mass relation, was systematically higher for interacting pairs. We find no difference with respect to interaction in the distribution of absolute magnitude (*top-right*) or redshift (*bottom-left*). While one could expect a bias in the classification, such that galaxies with brighter apparent magnitudes would have more visible debris, therefore increasing the fraction of “interacting” types, the distribution of apparent r-band magnitude shows no such trend (*top-right*). The distribution of interacting galaxies appears clearly biased towards smaller separations (defined as the ratio between pair separation and the half-light radius of the galaxy: R_p/R_e ; bottom-right).

3 COMPARING THE EMISSION LINE SPECTRA

Mergers and interactions disturb the gas in galaxies, and may lead to both AGN activity as the gas is driven towards the central supermassive black hole, or star formation if gas clouds can cool and collapse. Thus, identifying those galaxies which have undergone such activity in our sample will allow us to gauge the efficiency of this process in the specific case of gas-poor encounters between early-type galaxies. The identification of the ionising source in a galaxy is possible using emission line diagnostic diagrams (or BPT diagrams, see Baldwin et al. 1981). In this paper we use the standard BPT diagram juxtaposing the $[NII]/H\alpha$ and $[OIII]/H\beta$ line ratios (Veilleux & Osterbrock 1987). The classification scheme of galaxies according to this diagram is fully explained in Kewley et al. (2006) and is summarised below.

Star-forming galaxies are found below the Kauffmann et al. (2003) line:

$$\log([OIII]/H\beta) = \frac{0.61}{\log([NII]/H\alpha) - 0.05} + 1.3. \quad (1)$$

Galaxies above this line in the BPT diagram are likely to contain emission lines from an AGN. These galaxies are subdivided into two further sets: ‘Composite’ galaxies, possibly containing both an AGN and star forming regions, and galaxies whose ionisation spectra is dominated by AGN activity. Composite objects are those galaxies which lie above the Kauffmann et al. (2003) star formation line but below the theoretical upper limit of emission stimulated by star formation, namely (Kewley et al. 2001):

$$\log([OIII]/H\beta) = \frac{0.61}{\log([NII]/H\alpha) - 0.47} + 1.19. \quad (2)$$

Galaxies above this upper limit are said to have their emission dominated by an AGN. While it is possible to continue splitting the AGN population into Seyferts and LINERs, this adds little to our analysis, so it is omitted. Note that for a reliable classification, the four emission lines involved are required to have $S/N \geq 3$. We identify $\sim 20\%$ of our close pairs sample (~ 140 galaxies) as ‘active’ galaxies.

Table 1. Emission line classification for close pairs

Sample	Close Pairs		Interacting		Non interacting		Comparison ¹
	ALL	$R_P/R_e < 10$	ALL	$R_P/R_e < 10$	ALL	$R_P/R_e < 10$	
Number	695	140	467	41	228	99	15729
Quiescent	83.4%	79.3%	82.0%	76.8%	84.1%	85.4%	81.5%
Star Forming	3.9%	3.6%	2.2%	4.0%	4.7%	2.4%	4.3%
Composite	3.2%	1.4%	3.1%	2.0%	3.2%	—	6.9%
AGN	9.5%	15.7%	12.7%	17.2%	7.9%	12.2%	7.2%

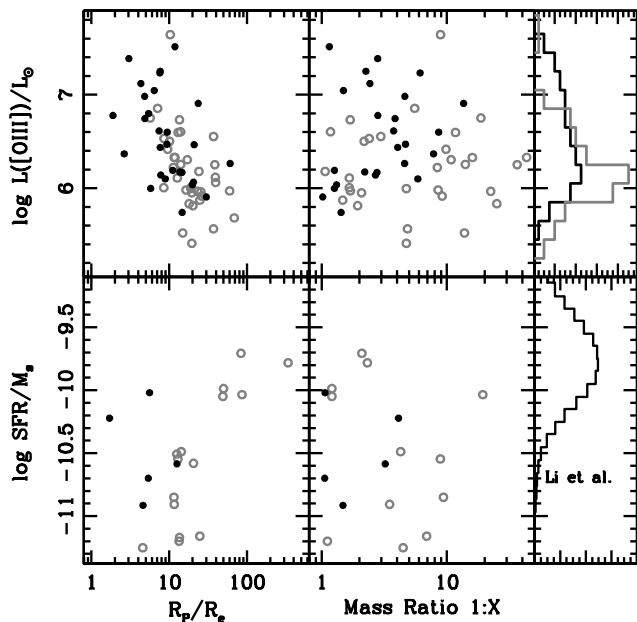
¹ The comparison sample is taken from Schawinski et al. (2007a).

Figure 4. *Top:* The luminosity of the [OIII] (5007\AA) line is shown with respect to the ratio between projected separation and half-light radius, R_P/R_e (*left*), and stellar mass ratio (*right*) of the Seyfert, LINER and unclassified AGN galaxies. Galaxies in pairs classified as interacting (non-interacting) are shown as black solid (open grey) circles, respectively. The histograms are colour coded in the same way. *Bottom:* Specific star formation rates with respect to the ratio between projected separation and half-light radius (R_P/R_e , *left*), and stellar mass ratio (*right*) for the star forming sub-sample. Galaxies in pairs classified as interacting (non-interacting) are shown as black solid (open grey) circles, respectively. The histogram is the distribution of specific star formation rates from the general sample of SDSS galaxies from Li et al. (2008).

3.1 Frequency of Active Galaxies

Shown in table 1 are the fractions of the sample with signs of AGN activity as a function of the pair interaction type. For a control sample of early-type galaxies we cannot use our original set of early-type galaxies (Rogers et al. 2007). That sample was extracted from Bernardi et al. (2006), which incorporates a colour cut in the selection, resulting in a bias on the number of active galaxies. Therefore we make use of a more general data set comprising morphologically classified early-type galaxies from Schawinski et al. (2007a), taken from SDSS DR4 and spanning a similar range in redshift. Figure 3 shows the dependence of emission line activity with respect to pair separation (R_P). The dashed lines illustrate the difference between the full sample (left side of each panel) and a subsam-

ple of close pairs, defined as those galaxies for which $R_P < 10R_e$ (right side of each panel). Short dashed lines show the Poissonian error bars. The control sample of Schawinski et al. (2007a) is given by a horizontal solid line in each panel. We also illustrate the dependence on signs of interaction: filled (open) circles correspond to galaxies classified as interacting (non-interacting). One can see that the differences between early-type galaxies in close pairs and in the control sample is quite small, but it appears to be more significant in systems with visual signs of interaction.

Previous studies have found an increased level of both star formation (Lambas et al. 2003; Alonso et al. 2004; Woods et al. 2006; Knapen & James 2009) and AGN activity (Alonso et al. 2007; Keel 1996) within close pair samples not segregated with respect to morphology. However, table 1 shows that restricting the analysis to early-type galaxies results in little or no significant difference – within Poissonian fluctuations – in activity between close pairs and the general population. This effect may be due to the lack of a substantial amount of gas in early-type galaxies to fuel either AGN activity or star formation. The small but non-negligible fraction of ‘active’ galaxies found both in a general and a close pairs sample could suggest that this activity is caused by a mechanism other than major mergers. A minor merger scenario (Kaviraj et al. 2009) could explain those fractions and the insensitivity to being in a close pair.

On the other hand, while the emission line properties of the overall close pair sample is consistent with a general sample, galaxies with visual signs of interaction show a higher fraction of AGN compared to both Schawinski et al. (2007a) and our non-interacting subsample. This result is significant within Poisson error bars. We note that the observed increase is in agreement with both Alonso et al. (2007), involving close pairs from SDSS, and Kaviraj (2009), who targeted Luminous InfraRed Galaxies (LIRGs). The underlying fractions in both samples are clearly dependent on the type of galaxy targeted, but the increase is consistent. The other point to notice is that the close pair early-type galaxies with visual signs of interaction also feature a lack of star formation. This is in contrast to previous studies on close pairs of all morphological types, which find a strong link between decreasing separation and increased star formation (see e.g. Alonso et al. 2004; Woods et al. 2006; Li et al. 2008). The interesting aspect is that the decrease in the fraction of star forming galaxies is coincident with an increase in the AGN fraction, a topic that will be discussed later on. Furthermore, the number of galaxies in the transition region between AGN and star formation (*bottom-right* panel of figure 3) decreases at small pair separation ($R_P < 10R_e$). Although speculative, one could envision those trends as an increase in AGN activity with decreasing pair separation.

Alternatively, it is possible that the signature of an increased black-hole accretion triggered by galactic interactions is damped by the presence of diffuse LINER-like emission that can masquerade

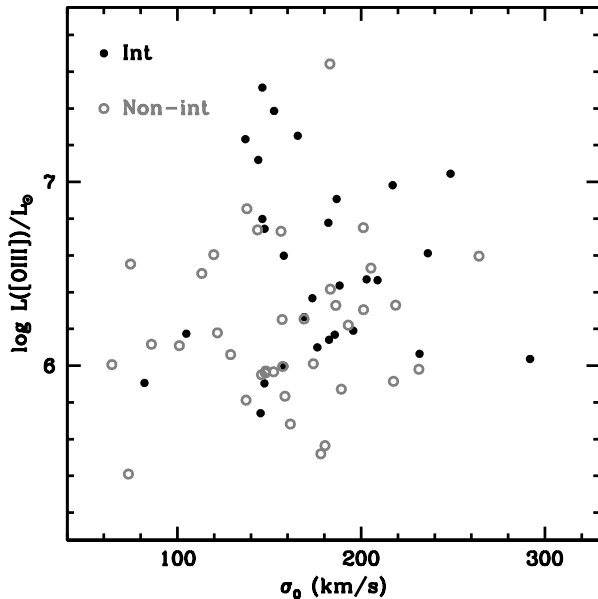


Figure 5. The luminosity of the [OIII] line as a function of velocity dispersion. The sample is segregated into interacting (black) and noninteracting (grey). We note that the interacting sample has an increased average luminosity but also that the correlation with mass is very weak for this sample.

as AGN activity, as recently suggested by Stasinska et al. (2008). This would be the case, in particular, if the power of such diffuse emission is limited by the amount of ionising photons produced by the old stellar populations that can reach the gas in early-type galaxies, rather than by the amount of such material.

3.2 Star Formation vs. AGN activity

To determine the possible effects of an increasing inflow of material into the centres of early-type galaxies in close pairs, we compare the star formation rate and the AGN activity from the luminosity of targeted emission lines. One would expect those to depend on the relative velocity, mass ratio or separation between galaxies. The star formation rate (SFR) is estimated from the luminosity of the $H\alpha$ emission line, using the standard correlation (Kennicutt 1998). In order to factor out the stellar mass, one can also define the specific star formation rate (i.e. the SFR per unit stellar mass) taking the stellar masses from the Garching catalogues (Gallazzi et al. 2005). The AGN activity can be traced using the luminosity of the [OIII] 5007Å line which scales with the bolometric luminosity of the AGN and thus the accretion rate of the central super-massive black hole (Heckman et al. 2004).

In figure 4 (*top*) we show the luminosity of the [OIII] line as a function of the separation (*left*) and the stellar mass ratio between the members of the pair (*right*). We only show those galaxies classified as pure AGN, since massive stars will also affect the luminosity of the [OIII] line, contaminating the interpretation of $L([OIII])$. The accretion rate is found to correlate with separation. The correlation holds even if we consider only the non-interacting pairs (grey open circles), which are overall found at separations $\gtrsim 10R_e$. This suggests that even in the absence of visual signs of interaction one

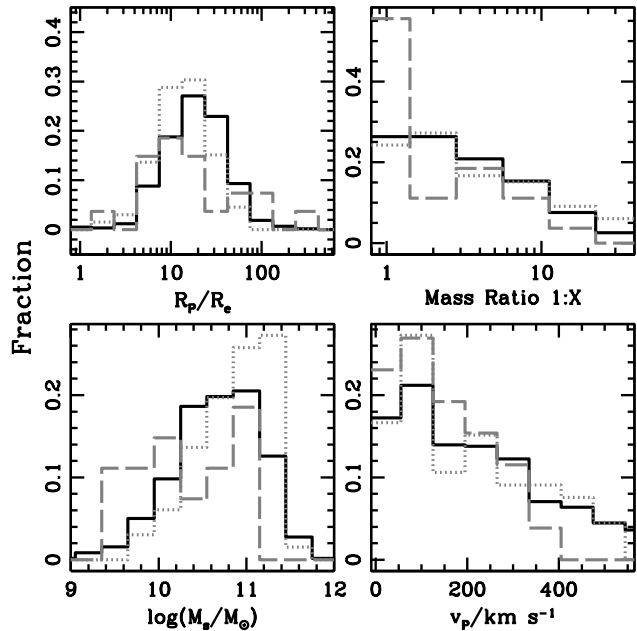


Figure 6. Sample properties when segregated with respect to emission line activity. The solid black, dashed grey and dotted grey histograms correspond to quiescent, star-forming and AGN galaxies, respectively.

could detect the effects of a close pair interaction from the activity of the central super-massive black hole. On the other hand, $L([OIII])$ does not correlate with the stellar mass ratio (*right*). The vertical histogram (*top-right*) illustrates the trend between visual signs of interaction and the activity of the central nucleus.

It is important to notice that this correlation does not reflect any bias regarding stellar mass. Shown in figure 5 is the luminosity of the [OIII] line as a function of velocity dispersion (i.e. a proxy for mass), we see that the increase of $L([OIII])$ due to the mass of the galaxy is minimal compared to the correlation seen in figure 4 with respect to pair separation.

As shown in table 1, only 4% of the total sample have emission lines consistent with star formation. Those galaxies are shown in the bottom panels of figure 4, where we present the specific star formation rate with respect to projected separation (*left*) or mass ratio (*right*). On the far right panel, the distribution of the specific star formation rate for the general sample of SDSS galaxies from Li et al. (2008) is given for comparison. As expected, our early-type close pairs sit at the low end of the distribution for a general sample. No significant trend is seen, although one could glimpse a correlation in the sample of non-interacting pairs (open grey circles) such that the specific star formation decreases with decreasing separation. Although weak, this trend fits with the increasing $L([OIII])$ as the pairs get closer, suggesting a transition from on-going star formation towards AGN activity.

Figure 6 shows the distribution of some properties of the sample when segregating with respect to emission line activity. The solid black, dashed grey and dotted grey histograms correspond to quiescent, star forming and AGN galaxies, respectively. Given the large differences in the number of galaxies belonging to each class, we show these histograms normalized to the number of members in each class. It is worth noting the strong correlation with respect to galaxy mass (*bottom-left*), with the AGN and star forming galaxies

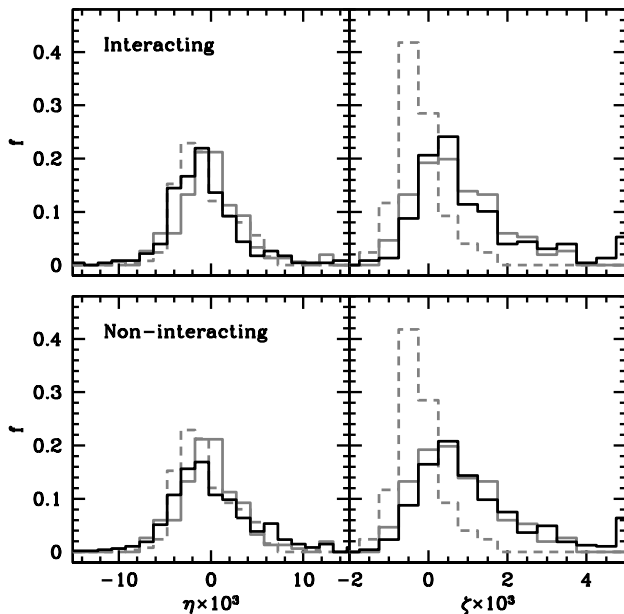


Figure 7. The distribution of the sample within η and ζ PCA space. The close pair sample (black histograms) is separated with respect to the visual classification: non-interacting (*bottom*) and interacting (*top*). For comparison, SDSS early-type galaxies with a GALEX detection are shown as grey histograms, with the dashed (solid) lines corresponding to red (blue) galaxies. The colour separation is based on the criterion for the presence of recent star formation, namely $\text{NUV}-r < 4.9$ for blue galaxies and $\text{NUV}-r > 5.9$ for red galaxies (see e.g. Kaviraj et al. 2007; Rogers et al. 2007).

dominating the top and bottom ends in stellar mass, respectively. The characteristic mass of a quiescent galaxy sits in between these two. Regarding mass ratios (*top-right*), we find a significant enhancement of star formation for more equal (but low-mass) ratios. This enhancement is also seen for lower relative velocities (defined as the difference between radial velocities; *bottom-right*).

4 COMPARING ABSORPTION LINE SPECTRA

In addition to AGN activity and ongoing star formation – which are processes triggered on shorter timescales – we also explore the effect of the interaction on the stellar populations as seen from the continuum and the absorption line spectra. In principle, one may not expect any significant changes in the properties of the bulk of the stellar populations during the first stages of an interaction (i.e. the phase we are only sensitive to in this sample). However, small and recent episodes of star formation can be detected in the optical spectra as shown in otherwise red and dead early-type galaxies (Rogers et al. 2007). Galaxies with recent but no on-going star formation will be excluded from the analysis in the previous section, based on the emission line spectra. Hence, by extending our analysis to the continuum and the absorption lines, we increase our sensitivity to detecting the effect of a close encounter between early-type galaxies. We consider two independent methods to determine differences in the stellar populations. The first one involves Principal Component Analysis (PCA), a model-independent technique aimed at extracting “directions” in a vector space spanned by the spectral data, along which the variation is maximal. A more con-

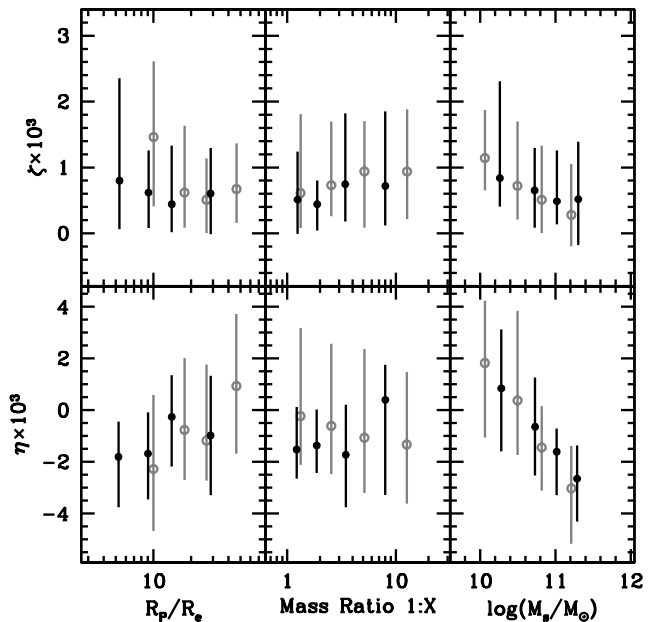


Figure 8. The parameters η (*bottom*) and ζ (*top*) derived from PCA are plotted as a function of the ratio between projected separation and half-light radius (*left*); mass ratio (*centre*) and stellar mass (*right*). The black solid (grey open) circles are averages for the pairs with (without) visual signs of interaction. The vertical lines span the 25th – 75th percentiles in each bin.

ventional second approach targets age-sensitive spectral features and compares them with a grid of models combined with population synthesis spectra to constrain the star formation histories (see e.g. Rogers et al. 2008).

4.1 Principal Component Analysis (PCA)

In order to maximally extract information from spectral data and to identify the smallest differences between them, we apply the method of Principal Component Analysis. It has proven to be a useful tool in the analysis of extremely homogeneous samples, as shown in Ferreras et al. (2006) and Rogers et al. (2007), where it was possible to identify small amounts of recent star formation at the level of a few percent in mass of ~ 1 Gyr old stars from the optical spectra.

We take the principal components (i.e. the basis “spectral vectors” on which the SEDs of these galaxies are projected) from a general (i.e. non close-pairs) sample of ~ 7000 early-type galaxies extracted from SDSS, previously defined and analysed in Rogers et al. (2007). We refer the interested reader to that paper for details of the method. This comparison set is a volume-limited sample extracted from the larger set of SDSS early-type galaxies defined in Bernardi et al. (2006), with the constraints: $M_r \leq -21$ and $z \leq 0.1$, with a further constraint on the signal-to-noise ratio of the spectra, $S/N \geq 15$ per pixel. This control sample provides us with the pre-processed basis spectra for the analysis (i.e. the principal components). After de-redshifting and correcting for Galaxy dust absorption, the spectra from the early-type galaxies in close pairs are then projected onto these eigenvectors, giving the pro-

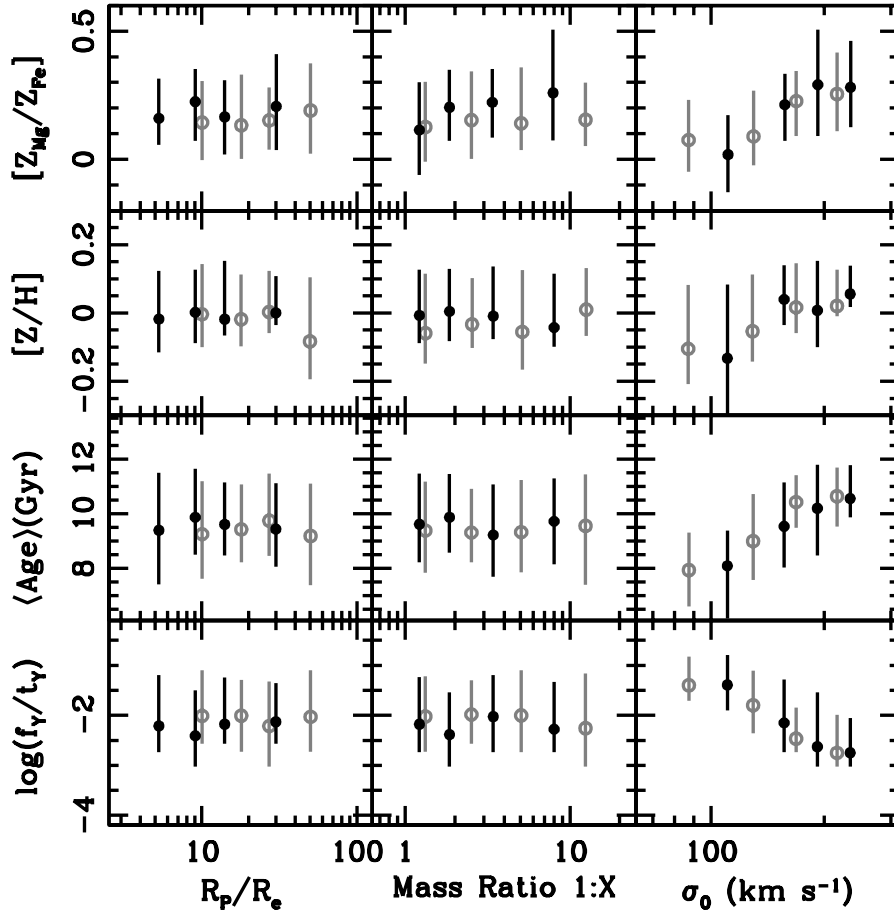


Figure 9. Best-fit stellar populations for a 2-burst model. The analysis involves a number of age- and metal-sensitive line strengths (see text for details). From top to bottom, the Mg-to-Fe ratio, metallicity, average age and the ratio between the young mass fraction and its age, are shown with respect to projected separation (*left*), mass ratio (*centre*) and central velocity dispersion (*right*). Solid black (open grey) circles correspond to galaxies with (without) visual signs of interaction. The vertical lines span the 25th – 75th percentiles of the distribution within each bin.

jected components (i.e. PC1, PC2) that quantify the relative weight of each eigenvector in the construction of the spectra:

$$\text{PC1}_i = \vec{\Phi}_i \cdot \vec{e}_1 = \sum_{j=1}^N \Phi_i(\lambda_j) e_1(\lambda_j), \quad (3)$$

and similarly for PC2, PC3, etc... While it is possible to determine the principal components straight from the close pairs data set, the smaller sample size means the extracted eigenvectors will be less robust. PCA relies on the variance of the data set to define an eigenvector and so large sets are preferred.

4.1.1 η and ζ components

The most successful mapping of PCA to extract information from the underlying stellar populations was found through the first two principal components. As shown in Rogers et al. (2007) these two components, PC1 and PC2, are consistent with an old and young stellar population, respectively. The eigenvector of PC1 shows a pronounced 4000Å break, significant metal absorption (e.g. H & K Ca II lines or a prominent G Band) and little or no Balmer absorption. In contrast, the eigenvector of PC2 features a blue continuum

with well-defined Balmer lines. The positive correlation between PC1 and PC2 (see figure 3 of Rogers et al. 2007), is likely caused by the relative values required to reconstruct the spectra (e.g. the shape of the continuum), which depends on the age and metallicity of the stars. Relative to this relationship between PC1 and PC2, a galaxy with a higher value of PC2 suggests the presence of a young sub-population. This idea was confirmed through a two-component stellar population model, in which the excess of the PC1-PC2 relationship was found to correlate with the mass fraction in young stars.

We also found a consistent correlation between the projections of the principal components and NUV photometry from GALEX. The NUV spectral region ($\lambda \sim 2300\text{\AA}$) is very sensitive to the presence of small fractions of young stars. The (NUV–r) colour has been shown to serve as an excellent indicator of recent star formation (Schawinski et al. 2007a; Kaviraj et al. 2007). We used GALEX photometry to define two subsets of galaxies, the first one is NUV bright (NUV–r \leq 4.9) and represents galaxies that have undergone recent star formation (within \sim 1Gyr). The second one is NUV faint (NUV–r \geq 5.9) and corresponds to an old, quiescent population. Rogers et al. (2007) showed that the projections of the principal components – *which only use the optical spectra* – could

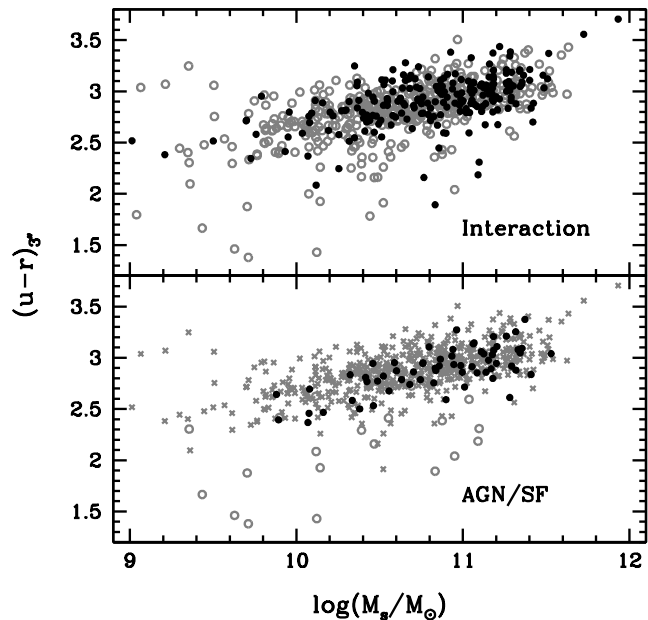


Figure 10. Colour-stellar mass relation of our sample. The colours are extracted from the SDSS DR7 database, dereddened and measured over the 3 arcsec aperture of the fibers used for the spectroscopy. The sample is divided with respect to visual signs of interaction (*top panel*) or emission line activity (*bottom*). In the top panel, solid black (grey open) circles correspond to galaxies with (without) visual signs of interaction. In the bottom panel, solid black (grey open) correspond to galaxies with AGN (Star-forming) activity. The grey crosses are quiescent galaxies.

be used to discriminate between these two populations of galaxies. Thus from the linear fit of the PC1 v. PC2 correlation, we define η as the distance along the relationship (sensitive to average age and metallicity) and ζ as the residual from this fit (sensitive to recent star formation).

4.1.2 Results

Figure 7 shows the distribution of components η (*left*) and ζ (*right*) for the close pairs (solid line histograms). The top (*bottom*) panels correspond to the interacting (non-interacting) visual type, respectively. In order to compare with a ‘control’ sample, we also show in each panel the histograms for the sample of (non-close pair) elliptical galaxies (Rogers et al. 2007), segregated with respect to NUV- r colour. NUV bright (faint) galaxies are shown as grey solid (dashed) lines. Both “interacting” and “non-interacting” galaxies have the same distribution of the η and ζ components. Thus, PCA indicates that there is little difference between the average populations of the two classes, which suggests that the visual level of disruption does not dictate the amount of recent star formation. Given these results it is not obvious that the interaction plays a significant role in shaping the stellar populations. This might be expected since our systems are the precursors of a dry merger. Furthermore, one could expect that the effect will not be apparent in the optical spectrum until later on in the merger.

However, from the histograms on the right-hand side of figure 7 one can see that the close pairs sample, both interacting and non-interacting, has a distribution of the ζ component consistent

with the general (i.e. non-close pairs) subsample of NUV-bright galaxies. This result indicates that elliptical galaxies in close pairs are more likely to contain small amounts of recent star formation than a general sample of early-type galaxies. It is acknowledged that this result could be due to the selection effects present in Bernardi et al. (2006). However, the dearth of close pair galaxies at the low end in the distribution of the ζ component means that this bias is unlikely. The distribution in the η component is not so useful to discriminate between quiescent spectra and recent star formation, although the figure shows that the close pair distribution sits ‘roughly’ in between the histograms for the NUV bright and faint galaxies. Given that η correlates with colour, one could conclude that studies purely based on broadband photometry cannot measure these differences. We note that these distributions are in agreement with previous work on early-type galaxies in Hickson Compact Groups, where a larger scatter towards high values of PC2 (roughly ζ) were found (Ferrerias et al. 2006).

In figure 8 we show the PCA components η and ζ as a function of pair separation (*left*); stellar mass ratio (*centre*) and stellar mass (*right*). The black solid (grey open) circles correspond to the interacting (non-interacting) pairs, and the vertical lines span the 25th – 75th percentile of the distribution in each bin. Out of the three observables, stellar mass is the only one that correlates significantly with the components, appearing redder (i.e. more negative η) towards higher masses. The correlation is much weaker with respect to ζ , which is the proxy for the presence of recent star formation. The mass ratio does not present any significant trend, and only the non-interacting pairs give a slight trend towards an increased recent star formation at small separations, although the scatter of the sample is rather large.

4.2 Modelling the Star Formation History

Since the close pairs sample has a higher mean value of the ζ component, we expect a large fraction of the sample to have undergone recent star formation. In order to quantify the effect on the underlying stellar populations, we explore a two-component star formation history. The synthetic spectra are generated from the 2007 stellar population models of Charlot & Bruzual (see e.g. Bruzual & Charlot 2003; Bruzual 2007), assuming a Chabrier (2003) initial mass function. The composite model superposes two simple stellar populations: an old component with age t_O , allowed to vary between 2 and 14 Gyr, with the metallicity between $\log(Z/Z_\odot) = -1.5$ and $+0.4$. A younger component of the same metallicity is added, with age t_Y , contributing a mass fraction, f_Y , which ranges from 0 to 0.5. The age of the young component is taken between 100 Myr and 2 Gyr. Note that the model grid contains a subset of models which are equivalent to standard simple stellar populations (i.e. $f_Y = 0$), such that a composite model will be chosen only if it improves the fit. Also note that the oldest ages considered (14 Gyr) are motivated by our choice of a standard Λ CDM cosmology ($\Omega_m = 0.3$, $H_0 = 70$ km/s/Mpc). The final grid of model consists of 65,536 star formation histories.

Our analysis follows the approach of Rogers et al. (2008), which involves multiple age-sensitive spectral features comprising three Balmer lines ($H\beta$, $H\gamma$ and $H\delta$) and the 4000Å break strength (D4000), along with a metal-sensitive index, [MgFe] (as defined in González 1993). Furthermore, a new definition of equivalent width (EW) is used, that significantly reduces the age-metallicity degeneracy over the traditional side-band method (see e.g. Trager et al. 2000). Our EWs are based on a new definition of the pseudo-continuum, determined from a (boosted) median of the surrounding

spectra and a 20Å spectral window centered on the line of interest. This definition has been shown to reduce the contamination of the pseudo-continuum from neighbouring lines, resulting in a less metal dependent H γ and H δ and a less age dependent [MgFe]. This method also provides smaller uncertainties in the EW at low S/N (Rogers et al. 2008).

While the BC03 models are not calibrated to accommodate non-solar abundance ratios, following Yamada et al. (2007) we use as a proxy the comparison between the best fit values of the metallicity when replacing in the analysis the metal-sensitive index [MgFe] by either $\langle \text{Fe} \rangle$ – defined as $0.5(\text{Fe}5270 + \text{Fe}5335)$ – or by the Mg*b* index. The difference in the metallicity derived from these two fits – labelled as Z_{Mg} and Z_{Fe} – is given as a crude estimation of the abundance ratio: $[Z_{\text{Mg}}/Z_{\text{Fe}}] \equiv \log(Z_{\text{Mg}}/Z_{\text{Fe}})$. The comparison of observed data and models is done via a standard maximum likelihood method. The errors for the EWs are estimated from Monte Carlo realizations of gaussian noise applied to the spectra. These errors are added in quadrature to the estimated systematic errors for the models (Bruzual & Charlot 2003).

4.2.1 Results

The results of the line strength modelling are shown in figure 9, as a function of projected separation (*left*); stellar mass ratio (*centre*) and central velocity dispersion (*right*). Black solid (grey open) circles correspond to close pair galaxies classified as interacting (non-interacting). The error bars give the 25th – 75th percentile range of the distribution within each bin. From top to bottom, we show the proxy for abundance ratio ($[Z_{\text{Mg}}/Z_{\text{Fe}}]$); metallicity; (mass-weighted) average age, and a quantity that gives the strength of the recent episode of star formation. The mass and age of the young population is degenerate, such that a small mass in young stars can be replicated by a larger mass fraction in older stars. Hence, we parameterise the effect on the spectra in terms of the ratio between the mass fraction in the young component to its age (f_Y/t_Y).

Consistently to the PCA studies described above, there is no significant difference between the stellar populations with respect to the visual presence of interactions. Furthermore, the populations are only sensitive to the velocity dispersion, a result already present in general samples of galaxies (see e.g. Bernardi et al. 2005). There is no significant trend with respect to separation or mass ratio. However, the modelling of the line strengths do reveal in an independent and consistent way to PCA that early-type galaxies in close pairs are more likely to have undergone recent star formation. We find 378 out of 695 galaxies (i.e. 54%) have a significant young population, $\log(f_Y/t_Y) \geq -2$, which is equivalent to 1% mass fraction of a 1 Gyr population.

The correlation between colour and stellar mass can also be used to understand the connection between pair morphology, emission line activity and the underlying stellar populations. Figure 10 shows the ($u - r$) colour-stellar mass diagram, where the colours are directly obtained from the SDSS DR7 database (de-reddened and measured within the 3'' aperture of the spectrograph fibers). In the top panel, solid black (grey open) circles correspond to galaxies with (without) visual signs of interaction. In the bottom panel, solid black (grey open) circles correspond to galaxies with AGN (star forming) activity. The grey crosses are quiescent galaxies. As expected, colour is strongly correlated with mass, which confirms the trend seen in the PCA components in figure 8. However, the departure from the red sequence – which is an indicator of younger stellar populations – does not depend on signs of visual interaction, agreeing with the PCA result of figure 7. However, with respect to

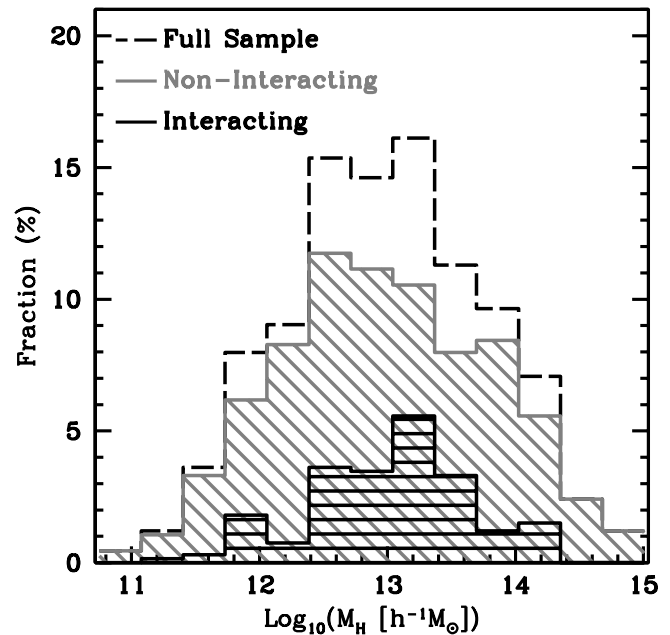


Figure 11. The distribution of the sample is shown in terms of estimated mass of the dark matter halo of the occupied galaxy group (M_H). The histograms show the distributions of the pairs depending on whether the system is visually classified as interacting (black solid) or not (grey). The full sample corresponds to the black dashed lines.

emission line activity (bottom panel of figure 10), we find a significant trend such that quiescent galaxies and AGN systems (crosses and solid dots, respectively) populate the red sequence, whereas galaxies with on-going star formation are identified as the members of the 'blue cloud'. The evolution from a weak star forming cloud towards a weak AGN and subsequently a quiescent galaxy has already been proposed elsewhere (Schawinski et al. 2007a). In the conclusion we apply this evolutionary path to the interpretation of the early-type close pairs.

5 ENVIRONMENT

We can also explore the properties of the close pairs with respect to environment. In order to assess the environment of a galaxy, we use the estimated mass of the host dark matter halo. This is determined through the group finding algorithm of Yang et al. (2005), which identifies galaxy groups starting with a friends-of-friends algorithm. The membership to these groups follows an iterative process controlled by the properties of the group and its halo. The application of this algorithm to a large sample of SDSS galaxies, forms the *galaxy groups catalogue* of Yang et al. (2007). The interested reader is directed to those references for an in depth description of the algorithm and catalogue. A cross correlation of this catalogue to our close pairs sample reveals a match to 664 of the 695 galaxies. As a measure of environment, we use the halo mass estimated based on the observed stellar mass of the group. We note that a more detailed investigation into the effects of environment as measured by the mass of the galaxy group halo is also underway on a much larger sample of ellipticals (Rogers et al. in preparation).

Figure 11 shows the distribution of our sample in terms of the host halo mass. The galaxies from our close pairs sample are mainly

located in intermediate mass halos of $M_H \sim 10^{13} M_\odot h^{-1}$. This is in agreement with the halo mass found by Pasquali et al. (2009) at which galaxies change from being preferentially star-forming to showing optical-AGN activity.

Our sample is clearly too small to map global properties of active early type galaxies, however it is interesting to see how the activity of the close pairs are affected. In a manner similar to Pasquali et al. (2009), we show in figure 12 the conditional fractions of galaxies classified as having undergone significant recent star formation (*top*) or split with respect to their star forming / AGN activity (*bottom*). The conditional fractions are given by the number of active galaxies within a bin of host halo mass divided by the total number of galaxies in that bin. The dashed lines towards the left of the figure represent the halos for which a considerable bias is expected towards low mass galaxies as imposed by the mass of the host halo. In addition to the limitation of galaxy mass by the group mass itself, it should be remembered that low mass halos preferentially host low mass galaxies (Yang et al. 2008). In a sample of this size it is difficult to overcome such a bias and this caveat should be considered alongside the conclusions of this section.

Figure 12 (*bottom panel*) shows that the fraction of galaxies classified as AGN is fairly constant¹ up to $M_H \sim 4 \times 10^{13} M_\odot h^{-1}$, above which there appears to be a rapid decline. The dearth of AGN galaxies at high halo masses is consistent with previous results Kauffmann et al. (2004); Gilmour et al. (2007); Pasquali et al. (2009). The exact reason for the cut off is not obvious but may be related to the reduction of gas available due to increased tidal stripping.

The fraction of star forming galaxies is higher in lower mass halos, although low mass galaxies – well known to have higher fractions of star-formation (Kauffmann et al. 2003) – dominate within these bins as mentioned above. The rest of the sample show a consistent fraction of star forming galaxies across all environment types. The number of galaxies is relatively small so a robust conclusion cannot be inferred, but it is interesting to note that no significant drop in star forming galaxies is seen with respect to halo mass.

Also shown in figure 12 (*top panel*), is the effect on the stellar populations where we consider how the amount of recent star formation is affected by the mass of the host halo. We define a “significant” amount of recent star formation as $S_Y \equiv \log(f_Y/t_Y) \geq -2$, or $\zeta \geq 10^{-3}$. The fraction of galaxies with RSF drops by $\sim 10 - 20\%$ as we move from low/intermediate to high halo masses. We note that this drop is qualitatively similar, although relatively higher, than that found in Schawinski et al. (2007b), which may be due to the high sensitivity of NUV or a function of the enhanced RSF already seen in the sample.

6 CONCLUSIONS

We have selected a sample of ~ 350 close pairs involving *only* early-type galaxies to measure environment effects. Through the use of emission line diagnostics, we classify $\sim 20\%$ of the sample as containing either an AGN or currently undergoing (weak) star formation. The fraction of these ‘active galaxies’ is consistent with an independent sample of early-type systems not in close

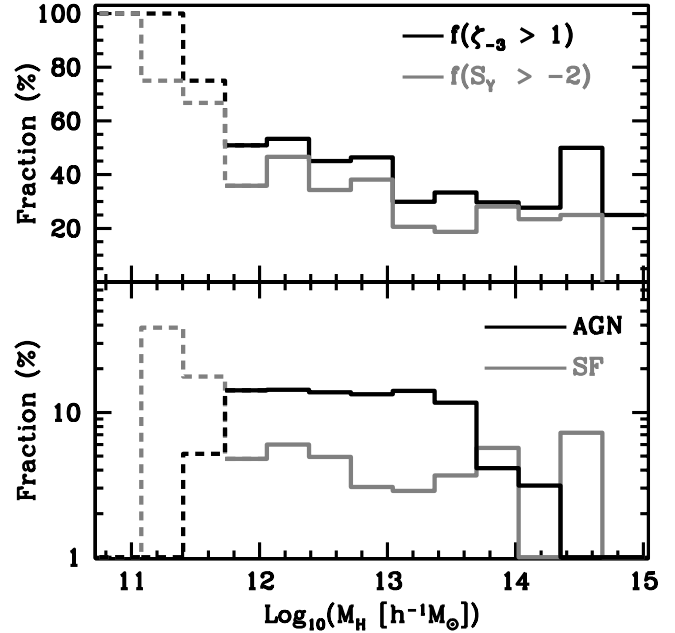


Figure 12. (*Top Panel*) The change in the fraction of galaxies with significant recent star formation as a function of the host halo mass (M_H). Shown for both PCA and SFH modelling results, where the significant level of RSF is defined by $\zeta_{-3} \equiv \zeta/10^{-3} \geq 1$ and $(S_Y =) \log(f_Y/t_Y) \geq -2$. (*Bottom Panel*) The fraction of galaxies containing AGN or star formation as a function of environment. The fraction are conditional, $f(AGN, SF|M_H)$, referring only to the galaxies contained within the specific halo mass bin. The solid grey and black histograms correspond to star-forming and AGN galaxies, respectively. The dashed line signify bins containing a bias towards low mass galaxies. It is interesting to note the drop in AGN fraction after $\log M_H \sim 13.6$ ($M_\odot h^{-1}$).

pairs, taken from Schawinski et al. (2007a). However, we found an excess of AGN and a lack of star forming galaxies in close pairs with visible signs of interaction. This result suggests that during the encounter, galaxies evolve from a (weak) star forming phase to an AGN phase. This idea is supported by the increase both in the AGN fraction and in the luminosity of the [OIII] (5007Å) line towards decreasing pair separation. Additionally, the specific star formation rate shows a hint of a decrease with decreasing separation, although the number of star forming systems is very low (contributing only 4% to the total sample).

A significant increase is found in the number of early-type galaxies in close pairs that have undergone a recent star formation episode, with respect to a control sample. This is shown both through PCA, where the close pair sample features high values of the ζ component (sensitive to young stellar populations), as well as by the line strength analysis using a grid of 2-component models, where a large proportion of the sample requires a significant amount of young stars. These two apparently contradicting scenarios – namely that the encounter appears to reduce ongoing star formation and the observation that the sample has increased levels of recent star formation – can be reconciled.

It is speculated here that the observed recent star formation is triggered during the first phases of the encounter by the interactions of the outer parts of the galaxies, including the dark matter halos. Since a large fraction of ellipticals have been found to contain HI and molecular gas, not only in their interstellar medium, but also in

¹ The small or zero fraction of AGN at low halo masses is most likely due to the lack of intermediate and high mass galaxies in these halos. However the increase in SF in these bins may hint that dust from such activity may obscure some of the AGN.

the form of satellite gas clouds (Knapp et al. 1989; Young 2005; Morganti et al. 2006; Combes et al. 2007; Donovan et al. 2007), the increasing gravitational perturbations induced by an oncoming neighbour will destabilise these clouds, driving them towards the galaxy (Sofue & Wakamatsu 1993; di Matteo et al. 2007). For instance, Li et al. (2008) found an enhanced star formation rate up to separations of 100 kpc on a large sample of SDSS galaxy pairs. Indeed the accretion of gas has been shown to instigate star formation even in early-type galaxies (e.g. Sofue & Wakamatsu 1993; Pipino et al. 2005; Khalatyan et al. 2008). The simulations of Khalatyan et al. (2008) suggest that the accretion of gas onto an early-type galaxy will be short lived due to the feedback from AGN.

As the pair comes closer – and within our selection criterion of $R_P < 30$ kpc – the increased gravitational interaction will enable the removal of angular momentum, driving gas towards the centre (see e.g. D’Ercole et al. 2000). Simulations from di Matteo et al. (2007) indicate that the greatest inflow of material to the centre occurs at separations ~ 10 kpc. Hence, at lower separations, most of the available gas is driven towards the centre, triggering the AGN activity and possibly quenching star formation. This is consistent with the simulations of Johansson et al. (2008), in which mergers between elliptical galaxies showed decreasing star formation rates with progression of the merger and rapid termination at the later stages coincident with increased black hole accretion. The feedback from the AGN in such cases should drive out the majority of the gas within the galaxy into the intergalactic medium. Given the high metallicity of early type stellar populations we might expect this to contribute to the abundance of the IGM.

Although speculative, this scenario explains the transition seen in the emission and absorption features of our sample, and is consistent with the observations of Schawinski et al. (2007a) on a general sample of early-type galaxies. Our results agree with the general study of SDSS close pairs of Ellison et al. (2008) who find that star formation also precedes AGN activity in close pairs of late-type galaxies.

The environment in which the interaction takes place also seems to affect the exact nature of the encounter. In low mass halos the initiated star formation appear to continue for longer into the interaction, i.e. to appear within our selection window of 30 kpc separation. The amount of recent star formation also appears to be higher in these low mass halos (possibly as a consequence) as well as in intermediate mass halos, which harbour most of the AGN activity. In contrast, halo masses greater than $M_H \gtrsim 4 \times 10^{13} M_\odot h^{-1}$ appear to have less AGN activity (almost none) and reduced amounts of RSF.

ACKNOWLEDGEMENTS

SK gratefully acknowledges a Research Fellowship from the Royal Commission for the Exhibition of 1851, a Senior Research Fellowship from Worcester College, Oxford and support from the BIPAC Institute at Oxford. This work has made use of the delos computer cluster in the physics department at King’s College London. Funding for the SDSS and SDSS-II has been provided by the Alfred P. Sloan Foundation, the Participating Institutions, the National Science Foundation, the US Department of Energy, the National Aeronautics and Space Administration, the Japanese Monbukagakusho, the Max Planck Society and the Higher Education Funding Council for England. The SDSS website is <http://www.sdss.org/>. The SDSS

is managed by the Astrophysical Research Consortium for the Participating Institutions.

REFERENCES

- Adelman-McCarthy, J. K. et al. , 2008, *ApJS*, 175, 297
 Alonso, M. S., Tissera, P., Coldwell, G., Lambas, D. G., 2004, *MNRAS*, 352, 1081
 Alonso, M. S., Lambas, D. G., Tissera, P., Caldwell, G., 2007, *MNRAS*, 375, 1017
 Baldwin, J. A., Phillips, M. M., Terlevich, R., 1981, *PASP*, 93, 5
 Bernardi, M., Sheth, R. K., Nichol, R. C., Schneider, D. P., Brinkmann, J., 2005, *AJ*, 129, 61
 Bernardi M., Nichol R. G., Sheth R. K., Miller C. J., Brinkmann J., 2006, *AJ*, 131, 1288
 Bell, E. F. et al. , 2004, *ApJ*, 608, 752
 Bruzual, G., Charlot, S., 2003, *MNRAS*, 344, 1000
 Bruzual, G., 2007, *ASPC*, 374, 303
 Bundy, K., Ellis, R. S., Conselice, C. J., 2005, *ApJ*, 625, 621
 Calzetti, D., 2000, *ApJ*, 533, 682
 Cappellari, M., Emsellem, E., 2004, *PASP*, 116, 138
 Chabrier G., 2003, *PASP*, 115, 763
 Combes, F. et al. , 1994, *ApJ*, 297, 37
 Combes F., Young L. M., Bureau M., 2007, *MNRAS*, 377, 1795
 Cox, T. J., Jonsson, P., Somerville, R. S., Primack, J. R., Dekel, A., 2008, *MNRAS*, 384, 386
 Davies, R. L. et al. , 2001, *ApJ*, 548, L33
 De Lucia, G. et al. , 2006, *MNRAS*, 366, 499
 D’Ercole, A. Recchi, S., Ciotti, L., 2000, *ApJ*, 533, 799
 di Matteo, P., Combes, F., Melchior, A.-L., Semelin, B., 2007, *A&A*, 468, 61
 Donovan, J.L., Hibbard, J.E., van Gorkom, J.H., 2007, *AJ*, 134, 1118
 Ellison, S. L., Patton, D. R., Simard, L. & McConnachie, A. W., 2008, *AJ*, 135, 1877
 Faber, S. M., Friel, E. D., Burstein, D., Gaskell, C. M., 1985, *ApJS*, 57, 711
 Ferreras, I., Pasquali, A., de Carvalho, R. R., de la Rosa, I. G., Lahav, O., 2006, *MNRAS*, 370, 828
 Ferreras, I., Lisker, T., Pasquali, A., Khochfar, S., Kaviraj, S., 2009, *MNRAS*, 396, 1573
 Gallazzi A. et al. , 2005, *MNRAS*, 362, 41
 Gilmour, R. et al. , 2007, *MNRAS*, 380, 1467
 González, J. J., 1993, Ph.D. thesis, Univ. California, Santa Cruz
 Heckman, T. et al. , 2004, *ApJ*, 613, 109
 Johansson, P. H., Naab, T., Burkert, A., 2008, *AN*, 329, 956
 Kang, X., van den Bosch, F. C., Pasquali, A., 2007, *MNRAS*, 381, 389
 Kauffmann, G. et al. , 2003, *MNRAS*, 341, 54
 Kauffmann, G. et al. , 2003, *MNRAS*, 353, 713
 Kauffmann, G. et al. , 2004, *MNRAS*, 353, 713
 Kaviraj, S. et al. , 2007, *ApJS*, 173, 619
 Kaviraj, S., 2008, *MPLA*, 23, 153
 Kaviraj, S., Peirani, S., Khochfar, S., Silk, J. , Kay, S., 2009, *MNRAS*, in press, arXiv:0711.1493
 Kaviraj, S., 2009, *MNRAS*, 394, 1167
 Keel, W. C., 1996, *AJ*, 111, 696
 Kennicutt, R. C., 1998, *ARA&A*, 36, 189
 Kewley, L. J., Dopita, M. A., Sutherland, R. S., Heisler, C. A., Trevena, J., 2001, *ApJ*, 556, 121

- Kewley, L. J., Groves, B., Kauffmann, G., Heckman, T., 2006, MNRAS, 372, 961
- Khalatyan, A., et al. , MNRAS 387, 13
- Khochfar, S., Burkert, A., 2003, ApJ, 597, 117
- Knapp, G. R., Guhathakurta, P., Kim, D.-W, Jura, M. A., 1989, ApJS, 70, 329
- Knapen, J. H., & James, P. A., 2009, ApJ, 698, 1437
- Kodama, T., Arimoto, N., 1997, A& A, 320, 41
- C. Li et al. , 2008, MNRAS, 385, 1903
- Lambas, D. G., Tissera, P. B., Alonso, M. S., Coldwell, G., 2003, MNRAS, 346, 1189
- Li, C., Kauffmann, G., Heckman, T. M., Jing, Y. P. , White, S. D. M., 2008, MNRAS, 385, 1903
- McDermid, R. M., et al. , 2006, MNRAS, 373, 906
- Morganti, R. et al. , 2006, MNRAS, 371, 157
- Morrissey P. 2005, ApJ, 619, L7
- Nolan, L. A., Raychaudhury, S., Kabán, A., 2007, MNRAS, 375, 381
- Naab, T., Khochfar, S., Burkert, A., 2006, ApJ, 636, 81
- Osterbrock, D. E. & Ferland, G. J., *Astrophysics of Gaseous Nebulae and Active Galactic Nuclei*, Sausalito, CA: University Science Books, 2006
- Park, C., Choi, Y.-Y., 2009 ApJ, 691, 1828
- Patton, D. R., Carlberg, R. G., Marzke, R. O., Pritchet, C. J., da Costa, L. N. , Pellegrini, P. S. 2000, ApJ, 536, 153
- Pipino, A., Kawata, D., Gibson, B. K., Matteucci, F., 2005, A&A, 434, 553
- Rogers, B., Ferreras, I., Lahav, O., Bernardi, M., Kaviraj, S. , Yi, S. K., 2007 MNRAS, 382, 750
- Pasquali, A., van den Bosch, F.C., Mo, H.J., Yang, X., Somerville, R., 2009, MNRAS, 394, 38
- Rogers, B., Ferreras, I., Peletier, R. F., Silk, J., 2008, astro-ph/0812.2029
- Sarzi, M. et al. , 2006, MNRAS, 366, 1151
- Schawinski, K. et al. , 2007, MNRAS, 382, 1415
- Schawinski, K. et al. , 2007, ApJS, 173, 512
- Sofue, Y., Wakamatsu, K., 1993, A&A, 273, 79
- Stanford, S. A., Eisenhardt, P. R., Dickinson, M., 1998, ApJ, 492, 461
- Stasińska, G., Vale Asari, N., Cid Fernandes, R., Gomes, J. M., Schlickmann, M., Mateus, A., Schoenell, W. , Sodr e, L. Jr., 2008, MNRAS, 391, L29
- Thomas, D., Maraston, C., Bender, R., Mendes de Oliveira, C., 2005, ApJ, 621, 673
- Tomita, A., Aoki, K., Watanabe, M., Takata, T., Ichikawa, S., 2000, AJ, 120, 123
- Trager, S. C. et al. , 2000
- Tremonti, C. et al. , 2004, ApJ, 613, 898
- van Dokkum, P. G. 2005, AJ, 130, 2647
- Veilleux, S., Osterbrock, D. E., 1987 ApJS, 63, 295
- Woods, D. F., Geller, M. J., Barton, E. J., 2006, AJ, 132, 197
- Yamada, Y., Arimoto, N., Vazdekis, A., Peletier, R. F., 2006, ApJ, 637, 200
- Yang, X.; Mo, H. J., van den Bosch, F. C., Jing, Y.P., 2005, MNRAS, 356, 1293
- Yang, X.; Mo, H. J., van den Bosch, F. C., Pasquali, A., Li, C., Barden, M., 2007, ApJ, 671, 153
- Yang, X.; Mo, H. J., van den Bosch, F. C., 2008, ApJ, 676, 248
- Yi, S. K. et al. , 2005, ApJ, 619, 111
- Young, L. M., 2005, ApJ, 634, 258